# Chemical Factors in Propellant Ignition

**Melvin A. Cook and Ferron A. Olson**
**University of Utah, Salt Lake City**

**A method of studying solid propellant ignition is described which utilizes detonating gas igniters. This article describes (1) conditions required for obtaining reproducible igniter systems and (2) results of application of the method to four well-known rocket propellants in which various "chemical" and "thermal" effects were brought out by suitable variations in the initial pressure and composition of the detonating gas igniter. Successful application of the detonating-gas-igniter method requires the use of steady state detonation waves, i.e., waves in which the detonation head has attained a steady "size" and momentum. Experimental data are presented which show that detonation (following the initial predetonation buildup) must travel 40 to 50 cm. in a 1-in. diam. steel tube before these steady state conditions are established in the systems studied.**

**Results of studies by the detonating gas ignition method show that, besides the important purely physical effects of temperature and pressure, free oxygen and solid carbon in the igniter system are very effective in lowering the threshold ignition pressure. Moreover, increasing oxygen in the igniter markedly lowers the ignition time lag ($\tau_p$) for appearance of an observable flame although it increases the time lag ($\tau_i$) for appearance of reaction sufficient to cause the first measurable ionization in the reaction zone ($\tau_p >> \tau_i$). Although true flame-ignition time lags were observed to be of the order of several milliseconds, reaction of the propellant was observed to start within 1 msec. (possibly immediately) after collision of the detonation wave with the propellant.**

**The detonating gas method is shown to provide a reliable measure of the relative ignition sensitivities of various rocket propellants.**

Chemical effects on propellant ignition may be defined as the effects exerted by various chemical species by virtue of specific chemical reactions, aside from the physical or "thermal" factors of temperature and pressure. It is important, however, to realize that the chemical effects described in this article require high temperature. Most investigations in propellant ignition have been concerned with the influence of temperature(*12, 24, 32*); pressure (*12*); and heat transfer by radiation(*1, 2, 20, 29*), convection(*13, 27*), and conduction(*18, 28*). The results of the few studies on chemical effects reported(*4, 13, 5, 27*) thus far have been inadequate to show conclusively that chemical effects are actually involved to an appreciable extent in propellant ignition, most investigators having attributed ignition primarily to the physical factors, temperature and pressure. One reason for uncertainty in this regard is that chemical factors have been studied at temperatures much lower than those encountered in practical ignition system. Also in many investigations, especially those with conditions comparing favorably with practical igniters, it was difficult to ascertain the composition of the gases actually contacting the propellant during the time interval between the initial application of energy and subsequent decomposition or burning of the propellant.

In an attempt to evaluate the specific or chemical influence of various chemical species on propellant ignition at realistic temperatures and pressures, a detonating-gas-ignition technique was developed. Detonating gases develop pressures and temperatures of the magnitude found in practical igniter systems, and these conditions may be varied reproducibly over relatively wide ranges by proper selection of the initial pressure and composition of the igniter system(*19*). Furthermore, the thermohydrodynamic theory of detonation, solved by use of the ideal gas equation of state, $pv = nRT$, known to be reasonably valid for gases(*26*), provides, in addition to the temperature, pressure, and other thermodynamic data for conditions existing in the detonation front(*15, 19*), the chemical composition of the products of detonation. Unfortunately detonation conditions prevail for only a few microseconds(*17*), whereas true ignition requires in general a much longer induction period. On the other hand, calculations show that the Chapman-Jouguet concentrations of the molecular species (i.e., the composition existing in the detonation wave) for the various igniters used here should maintain at least approximately during the entire ignition induction period. The detonation-head model, described in Appendix I, suggests that once the detonation wave has

This study was supported by U. S. Naval Ordnance Test Station Contract N123-60530S-1980. It comprises part of a thesis to be presented by Ferron A. Olson in partial fulfillment of the requirement for the degree of doctor of philosophy at the University of Utah.

propagated a length $L_m$, a steady state detonation head of constant size, momentum, pressure, and average particle velocity is attained. Consequently, according to this model thermodynamic conditions existing in the igniter gas from the wave front rearward should be relatively constant for a distance which should be equal to the distance covered by the wave front in about 10 to 20 μsec. Even though the ignition time lag is much greater than this, however, the most profound thermal effect on subsequent ignition should be that exerted during the time interval of application of detonation conditions owing to relatively sharp rarefactions and cooling outside the detonation head. Chemical effects on the other hand exert themselves over the entire induction period and are probably most important in the later stages.

The complete heat-balance equation of the propellant being ignited may be written as follows:

$$\alpha + \beta = \delta \qquad (1)$$

where the first term on the left ($\alpha = -K\nabla^2 T$) accounts for the heat conduction, the second term ($\beta = C\rho dT/dt$) for the heat content of the propellant, and the term on the right ($\delta = \rho Qk'f$) expresses the heat generated by chemical reaction of the propellant. (Here $K$ is the thermal conductivity, $\rho$ the density, $C$ the specific heat, $Q$ the specific heat of reaction, and $f$ a dimensionless function expressing the order of reaction.) Thus when ignition of propellants is accomplished with a detonating gas igniter, it is reasonable to assume that a relatively constant temperature corresponding to $T_2$ (the detonation temperature) persists at the propellant surface for the short period of application of detonation conditions (10 to 20 μsec.), during which term $\alpha$ is strongly positive, term $\beta$ increases rapidly in time, but term $\delta$ reaches importance probably only toward the end of this stage. The depth of penetration of heat into the propellant may be very small, possibly a few microns or less, but the surface should be raised essentially to gas-phase temperature. The increase in $\beta$ when $\alpha$ is positive starts reaction at the surface, and term $\delta$ increases exponentially in $T$, reaching a certain magnitude while $\alpha$ is still positive. During this phase both $\alpha$ and $\delta$ thus contribute to $\beta$ but $\alpha$ is of far greater importance. From considerations of the mechanism of burning of propellants (*12*) the first reaction involves only partial decomposition and is in general much less energetic than complete reaction. After the detonation head has passed beyond the propellant, the temperature of the surrounding medium drops rapidly; term $\alpha$ then becomes negative and heat flows outward from the now reacting propellant surface into the surrounding medium. (Sporadic positive thermal effects of the igniter after passage of the detonation wave exist owing to recurrent shock effects which are ever present, especially in short shot tubes, but may be reduced to negligible proportions by use of long shot tubes and careful control of the method of collision of the detonation wave with the propellant.)

The chemical effects described in this report are probably of very little, if any, significance during the part of the process where term $\alpha$ is positive. As soon as reaction has become appreciable, however, these chemical effects become important (1) by their influence on $Q$ in term $\delta$ and (2) by specific influences on the rate of reaction. While the surrounding medium will thus exert an adverse thermal influence on ignition after the detonation head has passed, or as soon as term $\alpha$ becomes negative, it may have a very pronounced positive chemical effect if it contains chemical substances which upon contacting the reacting surface can contribute to the heat and/or rate of reaction. Ignition or nonignition of the propellant will thus depend (1) on the magnitude of the energy input by the term $\alpha$ while the detonation head is in contact with the propellant and (2) on the later influence of specific chemical reactions between the gas phase and the propellant in the propellant reaction zone.

The detonating gas igniter method was for the reasons given above considered to offer promise as a means for studying propellant ignition.

## EXPERIMENTAL METHOD

### Ignition Threshold and Time Lag.

Quantitative data observable in the detonating gas ignition method for the study of propellant ignition include (1) ignition or nonignition and (2) ignition time lag. The most satisfactory index for ignition-nonignition is the minimum, or "threshold," pressure for ignition, where threshold pressure, designated $p_1°$, is here defined as the minimum initial pressure required to produce consistent ignitions of a given propellant by a particular detonating gas of given composition. A more fundamental index is, of course, the threshold detonation pressure $p_2°$. However, since $p_2$ may be computed from $p_1$ and $\rho_1$ through the hydrodynamic theory, $p_1°$ is quite as reliable an index as $p_2°$. It has the advantage of being a directly observable quantity where $p_2°$ is not. From numerous calculations made at this laboratory it was observed that for most of the igniter compositions used, many of the detonation properties were a linear function of log $p_1$(*7*). For example, in comparing a detonation property calculated at two different values of $p_1$, the following equation was found to hold satisfactorily. (*See* Figure 1.)

$$\psi_i''/\psi_i' = 1 + \beta_1 \log_{10} p_1''/p_1' \qquad (2)$$

where $\psi_i$ refers to any of the following thermodynamic variables: $Q_2$ (heat of explosion), $D$ (detonation velocity, $n_2$ (moles of detonation products/kg.), $T_2$ (detonation temperature), and some others not used in this study. Also $\beta_1$ is a different constant for each of the variables in question, and $p_1''/p_1'$ is the ratio of initial pressures.

The ignition time lag $\tau$ is defined as the interval between the initial application of energy to the propellant, i.e., impact of the propellant by the detonation front, and the time of ignition of burning of the propellant. The latter requires careful definition; it depends on the particular initial stage of burning one observes. Depending on how this "ignition" is observed, it may be identified with various stages of burning; for example, it may correspond to the first observable partial decomposition of the propellant, the initial observation of evolution of gas, or the initial appearance of a high-temperature, luminous flame. The literature describes three zones of propellant burning, namely foam, fizz, and flame zones(*30*). Each of these zones makes its appearance at a somewhat different time, and as a result observations involving different zones of burning would be described by different ignition time lags. One must, of course, exercise care to ascertain that the stage one is observing actually provides an adequate criterion of ignition, i.e., that a stable flame always appears at the particular stage observed.

One time-lag index employed in this study involved measurement of the induction period of initial decomposition sufficient to produce enough ionization for discharge of an ionization gap. This was determined by a technique(7) in which the time $\tau_i'$ to start decomposition and erode a given thickness $d$ of propellant from the surface of the exposed propellant face was measured. The real time lag $\tau_i$ corresponding to this index was then calculated from the equation

$$\tau_i = \tau_i' - d/k \qquad (3)$$

where $\tau_i'$ is the measured time and $k$ is the (pressure dependent) burning rate of the given propellant (30). Unfortunately $d$ could be determined only to within an accuracy of about 20 $\mu$, and the pressure was known only for the relatively short period of contact by the detonation head. Consequently the third term in Equation (3) was not known precisely. Since it turned out that under operating conditions $\tau_i << \tau_i'$, this criterion involved appreciable error. Moreover, there is some question whether $\tau_i$ may be considered as a true ignition index since true flame always appeared considerably later. However, it provides a means for detecting reaction in its early stages.

A relatively unambiguous definition of time lag is that based on the initial appearance of a stable flame $\tau_p$. This time lag, designated $\tau_p$, was determined by direct photography of the propellant face by use of either a streak or a Fastax camera. However, at $p_1$ values above 300 to 600 lb./sq.in. abs., depending on the igniter composition, the light from the detonation and recurring shock waves persisted a sufficient time to mask the initial appearance of the stable flame. Hence this method was applicable only at fairly low initial igniter pressures.

#### Equipment and Techniques

The results presented in this paper were obtained in three different heavy-walled, steel shot tubes all of 1-in. I.D. Initiation of the gas was effected in each case by the discharge of a 1-$\mu$f capacitor at 4,400 volts through a high-pressure (airplane) spark plug. Detonation and predetonation flame velocities were measured by means of the pin-oscillograph technique(7). Ionization gap pins were connected to separate capacitors charged to voltages of 250 to 1,700 volts (as desired). The capacitors were discharged in turn through the pin gaps by the highly conducting ionized wave front of the detonation or predetonation flame. This discharge was fed through suitable pulse-forming circuits to an oscilloscope, where it was recorded photographically as a "pip" on the calibrated sweep of an oscilloscope.

Shot tube I was 92 cm. long and was designed for pressures up to 30,000 lb./sq.in.abs. It contained ionization gap stages 50, 25, and 0 cm. ahead of the propellant to ascertain that a constant velocity was obtained at least 50 cm. before contact with the propellant. The propellant in this case was a smooth-surfaced 2.5-cm.-diam., 3-mm.-thick wafer and was mounted on the end of a plug that was threaded into the end of the tube opposite the point of initiation of the gas. Consequently the face of the wafer was perpendicular to the axis of the tube, and the detonation wave struck it broadside. Ignition was viewed in tube I through a plastic window sealed into the tube with O rings.

Shot tube I incurred difficulties associated with broadside collision of the detonation wave with the propellant, including excessive shock-wave interactions and complete interruption of the detonation wave. Despite these difficulties, results of threshold ignition measurement proved surprisingly reproducible, but the measurements of time lag were less satisfactory. Tube I served admirably in the preliminary evaluation of the detonating-gas-igniter method.

Shot tube II was designed to eliminate the undesirable features of shot tube I. It was a 1-in. I.D. tube 302 cm. long, capable of withstanding pressures up to 30,000 lb./sq.in.abs. The propellant was machined in the shape of truncated cones 7 mm. thick and 11 mm. in diameter at the apex. The propellant sample was forced into a conical hole in the side of the tube 107 cm. downstream from the igniter plug. In ignition threshold measurements the propellant face was allowed to crown out slightly into the bore as long as the edges of the pellet were not exposed. In measurements of $\tau_i$ the pellet face was machined flush with the tube walls by use of a spiral reamer. In either case the detonation wave could pass over the propellant without being appreciably disturbed, and consequently shock reflections back to the propellant occurred only later, at relatively long intervals. A 12.5-mm.-diam. window was located directly opposite the propellant pellet, allowing a direct view of the face of the propellant for photographing and manipulation. Also with tube II propellant wafers could be placed at one end of the tube just as in shot tube I, by means of which one could study the effect of the length of the column of igniting gas by comparison with results obtained in shot tube I.

In the measurement of $\tau_i'$ an ionization "pin" was located directly opposite the propellant to provide the time reference. The pellet pin, insulated except for a pointed end, was inserted through the plug holding the pellet in the tube wall into the back side of the pellet until the point was the desired distance $d$ under the pellet face. Adjusting the circuitry permitted the pips from each pin to be identified by variation in the voltages on the pins.

Shot tube III was designed for pressure up to 5,000 lb./sq.in.abs. primarily to study conditions required for the development of a steady state detonation head. It was 1.83 meters long and contained twenty-seven ionization gap stages, each of which could be interchanged with the igniter plug to enable one to ignite the gas at any desired position in the tube. Eighteen of these stages were spaced at 10-cm. intervals, and the remaining nine at 1-cm. intervals (spiraled around the tube) between the second and third 10-cm.-interval ionization-gap stages. Variable pip amplitudes were again used to enable one reliably to identify each pip with its respective ionization gap. This arrangement made possible the determination of the length $L'$ between the points of ignition and creation of the detonation wave and the variation of $L'$ with $p_1$ and composition. It also made possible the determination of the velocity of the flame front and its variation with distance $L$ (the total length of flame propagation from point of igniter gas ignition) in both the predetonation and detonation stages.

Pressures and total end impulse or momentum were measured by use of a dynamic condenser-type pressure gauge having a flat response between 0 and 10 kc., a resonant frequency of about 20 kc., and a 100% rise time of less than 50 $\mu$sec. It was located in the end of the tube opposite the igniter plug and thus received the full impact of the detonation head. The output of the pressure gauge was coupled to the vertical input of an oscilloscope, and the resulting sweep recorded a pressure-time curve.

The initial temperature of the igniter gas systems varied less than 15C.° in determination of $p_1$° for any particular propellant. Variations in the initial temperature of this magnitude have very little effect on the actual detonation conditions(26). Moreover, variation in the ambient temperatures seemed to have very little effect on ignition if held within this limit. The gases were used as received from the suppliers without further purification but were of about 99.5% purity.

Four homogeneous double-base rocket propellants, designated for security reasons as propellants *A*, *B*, C, and *D*, were studied. Each propellant

had about 50% nitrocellulose, approximately 30 to 40% nitroglycerine, and varying percentages of the usual plasticizers, stabilizers, and other additives. The propellant *C* had the highest nitroglycerine, and propellant *D* had slightly more nitroglycerine than *A* and *B*, which had equal amounts. Because propellant ignition seems to be dependent somewhat on the physical characteristics of the propellant, such as size, shape, and degree of roughness of the exposed surface, each of these factors was held constant in any particular series.

Composition of the igniter system was determined by the partial pressures admitting the gases into the mixing tubes separately. The gases were allowed to mix usually 10 min. or more in a mixing tank. All the shot tubes were thoroughly dried with an air nozzle, brushed with a wire brush, and then blown out with dry air after each shot. After evacuation of the shot tube the mixed gases were introduced from the mixing tank into the tube and allowed to remain there for 2 min. before firing.

### Thermohydrodynamic Calculations

By means of the thermohydrodynamic theory of detonation (*19, 26, 15*) the thermodynamic properties and the chemical composition at the Chapman-Jonguet plane were calculated for each of the igniter systems used. Calculations were made for each composition at three fugacities, corresponding approximately to the initial pressure $p_1$ of 1, 10, and 100 atm. Any desired thermohydrodynamic values in the range of 1 to 100 atm. could then be obtained very accurately by interpolation through Equation (2). These calculations are too extensive for presentation completely in this report but are available upon request. Some of the most important results for the $H_2$-$O_2$ system are given in Figure 1.

## EXPERIMENTAL RESULTS AND INTERPRETATIONS

### Detonating Gas System

Figure 2 shows comparisons of measured and calculated detonation velocities for the $H_2$-$O_2$ and $C_2H_2$-$O_2$ systems. The agreement between calculated and observed velocities was in general satisfactory, except in the $C_2H_2$-$O_2$ system for $C_2H_2/O_2$ mole ratios greater than 0.90, where the calculated velocities were higher than experimental. The experimental values agreed fairly well with those obtained by Breton (*26*) and Kistiakowsky and coworkers (*21, 23*). The discrepancy for high $C_2H_2/O_2$ ratios is attributed to failure to take into account all the important products of detonation. This problem has been discussed adequately by Kistiakowsky, et al., who computed detonation velocities in fair agreement with experiment for acetylene-rich $C_2H_2$-$O_2$ systems by making some further assumptions as to the detonation products and the mechanism of the reaction.

TABLE 1.—DISTANCE $L'$ FROM IGNITER TO POINT OF DETONATION FORMATION FOR THE $H_2$–$O_2$–A IGNITER

| Igniter composition ($H_2$-$O_2$-A (Parts by volume)) | $p_1$, lb./sq. in. abs. 12.5 | 25 | 50 | 75 | 100 | 150 |
|---|---|---|---|---|---|---|
| 1-3-0 | — | 127 | 121 | 112 | 107 | 101 |
| 1-2-0 | 75 | 65 | 56 | — | 52 | 45 |
| 1-1-0 | — | 40 | 29 | 27 | 20 | 20 |
| 2-1-0 | 31 | 20 | 13 | 16 | 15 | 10 |
| 3-1-0 | 42 | 23 | 22 | 15 | 17 | 12 |
| 4-1-0 | 64 | 58 | 48 | 41 | 39 | 37 |
| 6-1-0 | — | 116 | 112 | 94 | 108 | 99 |
| 2-1-½ | 25 | 15 | 17 | — | — | 15 |
| 2-1-1 | 24 | | | | | |

The $L'$ vs. $p_1$ and composition results for the $H_2$-$O_2$ and a portion of the $H_2$-$O_2$-A system are shown in Table 1.

$L'$ was determined with tube III from measurements of the average velocity of the flame front between

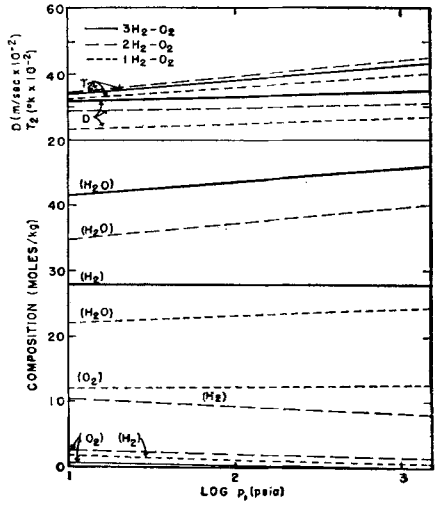


Fig. 1. Variations of theoretical detonation composition, temperature $T_2$ and velocity $D$ with initial pressure $p_1$ and initial composition for the $H_2$-$O_2$ igniter system.

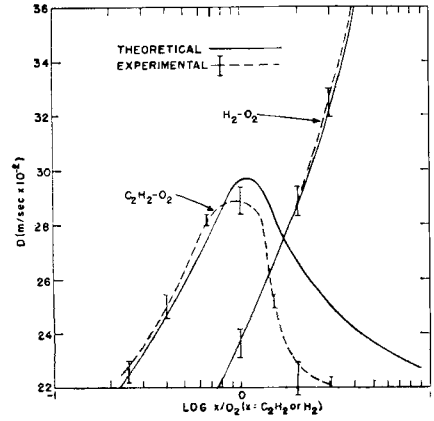


Fig. 2. Variations of theoretical and experimental detonation velocity with initial composition for the igniters $C_2H_2$-$O_2$ ($p_1 = 2$ atm.) and $H_2$-$O_2$ ($p_1 = 1$ atm.).

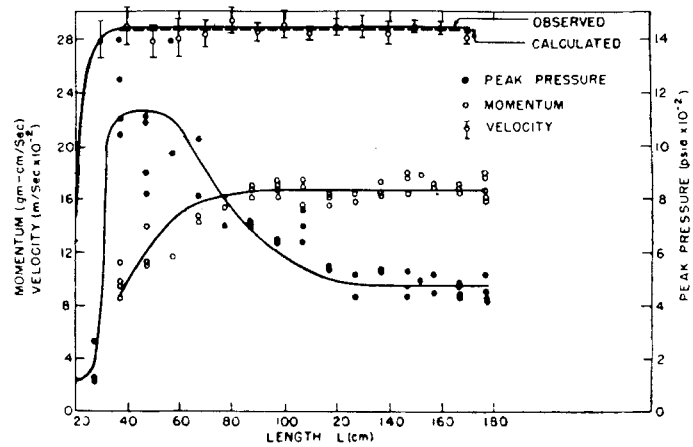


Fig. 3. Momentum, velocity, and peak pressure vs. length for the system $2H_2$-$O_2$ at 12.5 lb./sq. in. abs. (tube III).

ionization-gap stations. The data given are subject to a possible error of about ± 2 to 10 cm., being greater for large values of $L'$. $L'$, like the thermohydrodynamic variable mentioned above, seemed to show a linear relationship with log $p_1$. As was expected, the most energetic compositions in the region of $2H_2$-$O_2$ (2-1) (compositions being expressed throughout in parts by volume) showed the minimum value of $L'$, although 3-1 and 1-1 exhibited only slightly larger values of $L'$.

Velocity-distance ($D$-$L$), peak-pressure–distance ($p$-$L$), and end-impulse - or - momentum–distance ($M$-$L$) relations obtained in shot tube III with $2H_2$-$O_2$ are shown in Figure 3.* It will be observed that steady state momentum was established at about 80 cm. from the point of ignition of the gases, although 120 cm. of propagation was required for the attainment of a steady state peak pressure. $L'$ was about 30 cm.

As mentioned, solid explosives show a steady state detonation head of constant size and momentum for $L_m > 3.5d$. Also $L_m$ is dependent primarily only on the geometry of the charge and not on the initial density and composition. The momentum vs. $L$ results for the mixture $H_2/O_2 = 2$ given in Figure 3 show that a steady state detonation head is also established in gaseous detonations in this case for $L_m \sim 50$ cm. Studies are in progress for the other systems but are as yet incomplete. It is expected that they will confirm the suggestion of the detonation-head model that $L_m$ should be relatively insensitive to composition and density. In such a case steady state detonation should have been attained at the position of the propellant in both tubes I and II for all $H_2$-$O_2$ compositions in the range $1 < H_2/O_2 < 4$. In all cases $L'$ was less than 42 cm. for these igniters. These conclusions seem to be substantiated by curves (2) and (3) (Figure 8), which are comparisons of plots of $p_1°$ vs. $H_2/O_2$ data obtained in shot tubes I and II. (*See* below.)

For the $C_2H_2$-O igniter systems (Figure 2) detonation occurred after a flame propagation of less than 42 cm. ($L' < 42$ cm.) for all compositions in the range $0.2 < C_2H_2/O_2 < 1.5$. The upper limit, however, is somewhat uncertain owing to the formation of excessive free carbon in this range which caused erratic behavior of the pin-oscillograph equipment. Detonation should thus have been steady in this system at the position of the propellant in both shot tubes.

Although not a great deal is known concerning the limits of detonation of the $H_2$-$O_2$-$N_2$ and the $H_2$-$O_2$-A igniter systems, it appears unlikely that steady state detonation was established in shot tube I for the 2-3-$X$ ($N_2$ or A) systems, although steady state detonation was probably developed in the 4-1-$X$ ($N_2$ or A) systems for small values of $X$. With the 2-1-$X$ ($N_2$ or A) igniters the steady state occurred possibly for $X$ as high as 40%.

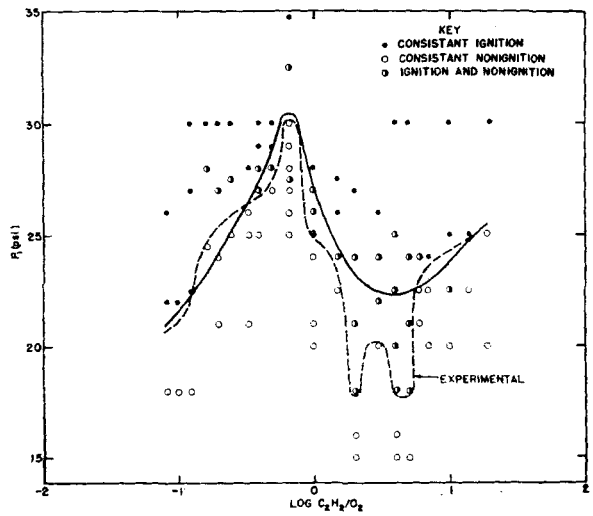


Fig. 4. Threshold ignition pressures $p_1°$ vs. igniter composition for propellant A in shot tube I.

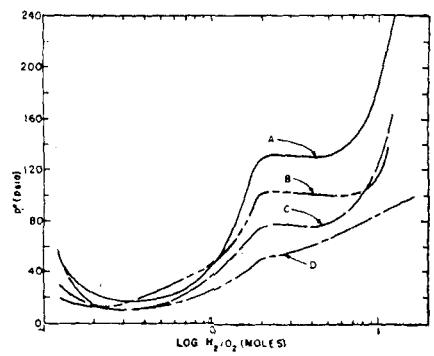


Fig. 5. Threshold ignition pressures $p_1°$ vs. igniter composition for propellants $A$, $B$, $C$, and $D$ in shot tube I ($H_2$-$O_2$ igniter).

*Experimental velocities of 2,819 and 2,821 meters/sec. were obtained by Lewis (25) and Bone (3) respectively.

**Ignition-threshold Pressures**

Figure 4 is a plot of the logarithm of the mole ratio $C_2H_2/O_2$ vs. $p_1°$ for propellant A. The broken line gives the ignition-threshold curve as a function of composition. However, it is doubtful that the results were sufficiently consistent to justify the detailed broken curve; the solid curve is considered to be the best smooth curve through the observed data. The threshold pressure curve showed a maximum for the 2-3 ($C_2H_2$-$O_2$) igniter and decreased sharply on both sides. Powdered carbon was found in minute quantities with the igniter 1-1 ($C_2H_2$-$O_2$); it increased rapidly to copious amounts as the proportion of the acetylene in the igniter was increased. These results show that both oxygen and solid carbon are effective in enhancing ignition of propellants.

The $p_1°$-vs.-composition curves for the propellants $A$, $B$, $C$, and $D$, achieved by means of $H_2$-$O_2$ igniters, given in Figure 5 were obtained from 300 tests at eight different $H_2/O_2$ ratios between 0.125 and 12.0. The data were too extensive for each point to be shown, but they were quite consistent, and the curves may thus be considered as a reliable representation of the experimental data. They show in general large $p_1°$ values for the hydrogen-rich igniter and quite small $p_1°$ values for the oxygen-rich igniters. While all propellants showed marked sensitivity to excess oxygen in the products of detonation, propellant $A$ appeared somewhat more sensitive to oxygen than propellant $D$. From Table 1 and Figure 5 it may be seen that detonation was produced in shot tube I only in the igniter composition range $H_2/O_2$ from 0.4 to 5.0, and the failure of $p_1°$ to increase sharply with $H_2/O_2$ from 5 to 7, even though these igniters did not detonate, indicates that the deflagaration flame, although cooler and less intense than the detonation flame, is at least as effective as the detonating gases in igniting the propellant. With the extremely hydrogen-deficient and hydrogen-rich igniters the curves were very steep, except for propellant $D$ at $H_2/O_2 = 12.0$. This steep rise may be due to the re-

duced temperature of the flames as the limits of inflammability were approached (*26*).

The ignition-threshold method used with igniters with little or no oxygen or solid carbon clearly differentiated the relative sensitivities of the propellants. On the oxygen-rich side the sensitivities differed very little, owing to the large oxygen effect. Hence the measurement of relative ignition sensitivity should be confined to a particular composition in which $(O_2)$ is small or absent, for example, $2H_2$-$O_2$.

Ignition-threshold pressures of propellant *B* in shot tube I resulting from use of igniter systems 2-3-$XN_2$ and 4-1-$XN_2$ ($H_2$-$O_2$-$N_2$), 2-3-*XA*, 2-1-*XA*, and 4-1-*XA*, where $XN_2$ and *XA* refer to the mole ratio of nitrogen and argon in the igniter system, are summarized in Figures 6 and 7. The percentage of nitrogen and argon was varied from 0 to 70 mole %. It was thought that the initial decrease in $p_1°$ with $N_2$ might be associated with oxides of nitrogen and that therefore the substitution of argon for $N_2$ would change the shape of the curves considerably. Instead the comparable sets of curves proved to be surprisingly alike. It is possible that the reduced heat capacity of the argon systems produced approximately the same trend as oxides of nitrogen in the nitrogen systems. In nearly all cases the curves exhibited more than one minimum. The maximum percentage of nitrogen at which detonation was obtained in shot tube I is not known accurately but was limited to less than 40% as judged from the disappearance of the characteristic "ping" at this percentage of nitrogen. Hence the minima observed at about 50% may be associated with the change from detonation to deflagration and finally to simple quiescent burning. Incomplete studies of the ignition thresholds of propellants *A* and *C* were also made with the igniters $2H_2$-$O_2$-$XN_2$ and $H_2$-$O_2$-$XN_2$. They too exhibited the characteristic minima which seems to be associated with change in the burning mechanism.

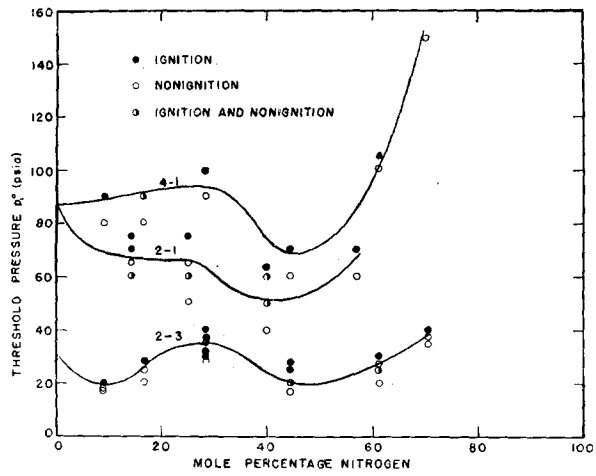


Fig. 6. Threshold ignition pressure $p_1°$ vs. percentage of nitrogen for propellant *B* at $H_2/O_2 = 4$, 2, and 0.67 (shot tube I).

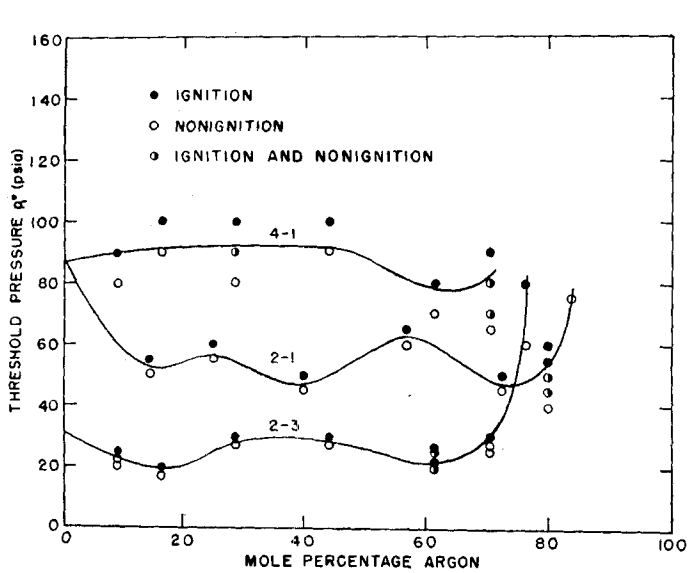


Fig. 7. Threshold ignition pressure $p_1°$ vs. percentage of argon for propellant *B* at $H_2/O_2 = 4$, 2, and 0.67 (shot tube I).

Figure 8 gives a comparison of $p_1°$-vs.-composition curves of propellant *C* obtained in shot tubes I and II with the $H_2$-$O_2$ igniter system. Curve (1) was obtained in tube. I. For this curve the gases were mixed in the tube for at least 10 min. Curve (2) was also drawn from data obtained in tube I, but the gases were premixed at least 30 min. in the mixing tank. The two curves agree fairly well except for a decrease in $p_1°$ for $H_2/O_2$ above 2. The data for curve (3) were obtained under exactly the same conditions as (2) but in shot tube II. It is believed that all compositions in the range $3.0 > H_2/O_2 > 1.0$ should have attained a steady detonation head at $L << 302$ cm. It may be noted that the curves are similar in shape but differ by a fairly constant value of about 60 to 70 lb./sq.in.abs., indicating that the same steady state detonation conditions existed in the 92-cm. tube as in the 302-cm. tube for this system. These results illustrate the importance of recurrent shocks in shot tube I. Data for curve (4) were also obtained in tube II, but in this case the propellant pellet was placed in the side of the tube 107 cm. from the point of igniter ignition. Here $p_1°$ for $H_2/O_2 = 2$ was about double that of curve (3), where the propellant wafer was at the end of the tube and interrupted the detonation wave directly, but at $H_2/O_2 = 1$ for glancing incidence $p_1°$ was much less than was obtained for broadside collision with the detonation wave.

The most significant result of the ignition threshold studies with $H_2$-$O_2$ mixtures is the marked influence of oxygen on threshold pressure $p_1°$.

Figure 9 shows plots of all the pertinent (calculated) detonation properties at the threshold pressure $p_1°$ against the $H_2/O_2$ ratio together with the experimental $p_1°$-vs.-$H_2/O_2$ plot itself. This figure brings out clearly this oxygen effect. $(O_2)$ refers to the concentration of free uncombined oxygen, in

mole per cent, in the detonation head.) The threshold pressure was eight times greater for the maximum temperature composition $2H_2$-$O_2$ than for one of 20% lower temperature but about ten times higher $(O_2)+(O)$ content. Figure 10, in which the index $1/p_1°$ (instead of $p_1°$) is plotted against $C_2H_2/O_2$, shows in a striking manner the influence of $(O_2)$ and $(c_s)$, concentrations which considerably outweighed even the temperature involved. (It is $1/p_1°$, not $p_1°$ which should parallel relative ignition sensitivity.)

### Ignition Time Lag

Table 2 gives values of $\tau_i'$ obtained with propellant $C$ and various $H_2$-$O_2$ systems. Negative values of $d$ denote results in which the pellet pin protruded completely through the propellant pellet face into the chamber of the tube. In these cases pips were observed on arrival of both the detonation wave and the first reflected shock,

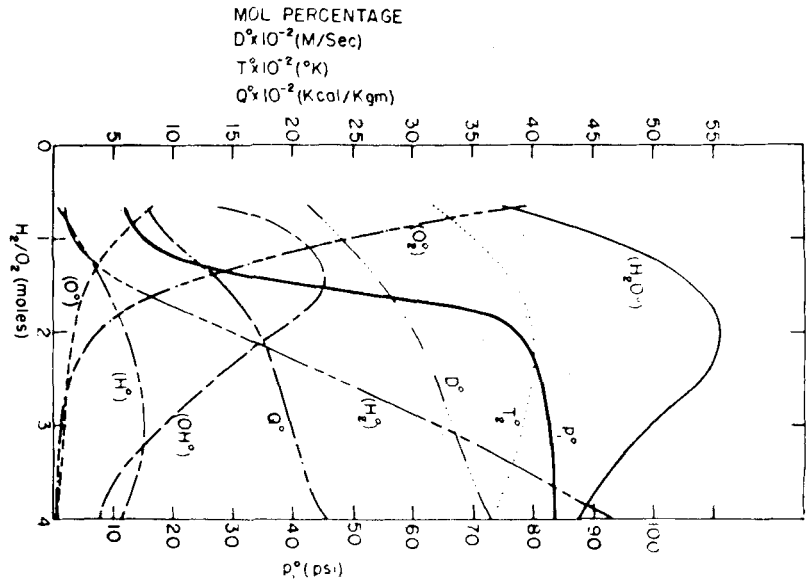


Fig. 9. Comparison of threshold detonation conditions ($D°$, $T_2°$, $O_2°$, etc.) for propellant $C$.

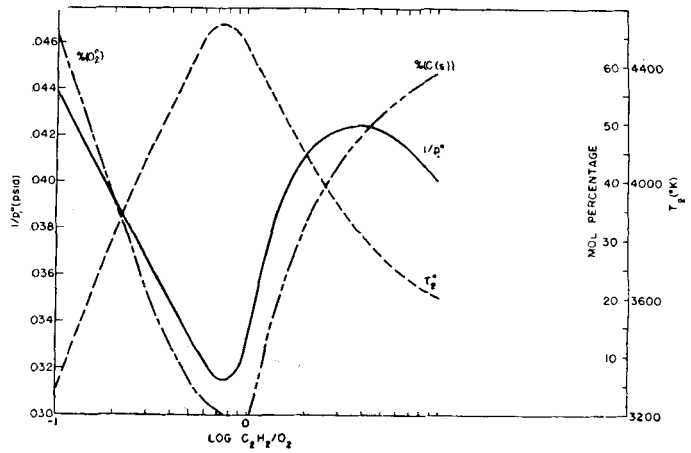


Fig. 10. Comparison of threshold detonation conditions ($T_2°$), ($O_2°$), and ($C_s°$) with $1/p_1°$ for propellant $A$.

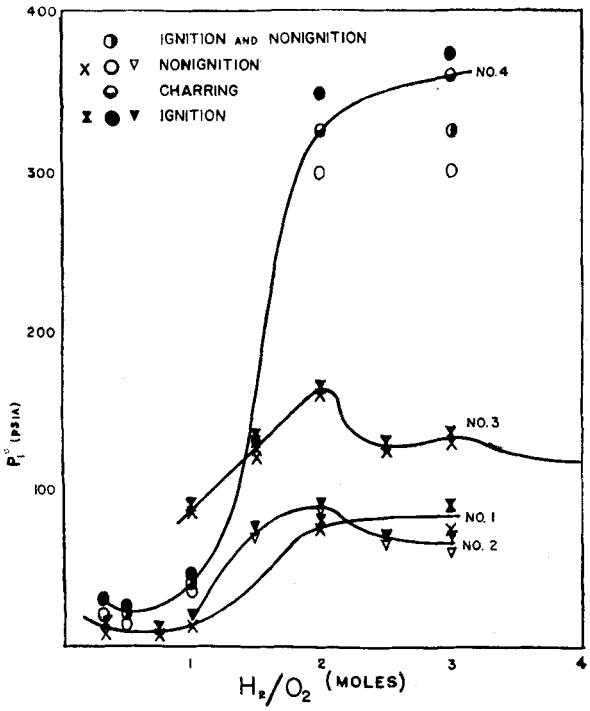


Fig. 8. Comparison of threshold pressures in shot tube I (curves 1 and 2) and shot tube II (curves 3 and 4) for propellant $C$ ($H_2$-$O_2$ system).

TABLE 2.—DATA ON $\tau_i'$ FOR PROPELLANT $C$ WITH THE $H_2$-$O_2$ IGNITER AT 300 LB./SQ. IN. INITIAL PRESSURE

| $H_2$–$O_2$ | | $H_2$–2 $O_2$ | | $H_2$–4 $O_2$ | |
|---|---|---|---|---|---|
| $d$, $\mu$ | $\tau_i'$, msec. | $d$, $\mu$ | $\tau_i'$, msec. | $d$, $\mu$ | $\tau_i'$, msec |
| 750 | 59.40 | 10 | 4.65 | 95 | 13.27 |
| 400 | 18.20 | 0 | 2.52 | 90 | 16.40 |
| 200 | 8.80 | 0 | 2.52 | 60 | 3.98 |
| 85 | 6.25 | 0 | 2.50 | 50 | 4.11 |
| 75 | 6.80 | −5 | 2.50 | 10 | 5.03 |
| 50 | 2.02 | | | 0 | 2.70 |
| 30 | 2.11 | | | −40 | 2.70 |
| 10 | 2.13 | | | | |
| 10 | 2.05 | | | | |
| 0 | 2.13 | | | | |
| −30 | 2.11 | | | | |

the time being sufficient for the pins to recharge. Even though the pellet pin was exposed directly to the gases in the tube, the ionization gap did not break down a second time until the first reflected shock wave crossed the pellet face. The recurrent shock did not cause breakdown of the pellet gap when the pellet pin was not exposed, i.e., for a pin still buried in the pellet. It was possible to ascertain this from the fact that the pip furnished by the pellet gap was much larger than that from the reference pin. Also at $d \geqslant 75, \geqslant 10$, and $\geqslant 10$ $\mu$, respectively, for the igniters 1-1, 1-2, and 1-4, the first shock failed to cause pellet-pin breakdown, as shown by the $\tau_i'$ values obtained for these values of $d$.

From the data in Table 2, with $p_2$ as the upper limit of $p$ during reaction and the known burning-rate law of propellant $C$, the upper

limit of $\tau_i'$ was computed to be 1.1 msec. Since the pressure was much lower than $p_2$, $\tau_i$ must have been much less than 1.1 msec. Similarly, $\tau_i$ was much less than 2.5 msec. for propellant *C* when the 1-2 and 1-4 igniters were used.

The meager data obtained so far for $\tau_p$ are given in Table 3. They indicate that the true ignition time lag is directly dependent on the initial pressure and inversely dependent on the percentage of oxygen in the igniter; i.e., $\tau_p$ varied linearly with the mole ratio $H_2/O_2$, extrapolating to 260 msec. for $\tau_p$ at $H_2/O_2 = 2.0$. As expected, $\tau_p$ was much larger (seventeen times as large for the igniter 2-1) for glancing than for broadside collisions of the detonation wave with the propellant.

From tables 2 and 3 and observed $\tau_i$ and $\tau_p$ data it appears that (1) reaction is initiated within about 1 msec. and possibly within a few microseconds if not immediately after the detonation front strikes the propellant, (2) the time to start the initial reaction apparently is highly temperature dependent and not appreciably dependent on the chemical effects, (3) stable ignition occurs several milliseconds later, and (4) stable burning is initiated more rapidly in the presence of oxygen. Presumably (4) would be true also of solid carbon but no measurements of time lag have yet been made to determine this. In normal burning of propellants three stages of reaction have been observed, namely foam, fizz, and flame(*30*). The ordinarily slightly exothermic (or perhaps even endothermic) foam stage consists of partial decomposition of the large polymers in the propellant to large molecules which remain on the surface. The fizz stage consists evidently of the initial formation of gaseous products. This stage is exothermic nearly to the extent of the very hot flame stage, where the propellant reactions go to completion. Application of this burning theory to the time-lag results indicates that the foam stage may occur within a very few microseconds after the very intensive energy source, the detonation head, is applied and that $\tau_i$ may measure a stage in the initial formation of the fizz zone. In the formation of the foam zone one requires a strong supply of heat. The reaction becomes strongly exothermic only after the fizz zone has developed sufficiently. Apparently collision of the detonation head with the propellant produces the foam zone and early stages of the fizz zone. Only after a time $\tau_i$ has the fizz zone developed sufficiently to produce enough ions for discharge of the pins of the pin oscillograph. During this stage thermal effects are much more pronounced than the chemical effects discussed in this report. This is in accord with the observation that $\tau_i$ increases with the oxygen content (or more fundamentally with decreased temperature) for $H_2$-$O_2$ igniter systems of positive oxygen balance.

Chemical effects on ignition are limited to the fizz zone and possible even to the later stages of development of this zone. This would account for the strong inverse oxygen dependance of true flame ignition time lag $\tau_p$. It would also account for the decreasing threshold pressures found for igniters with increasing oxygen content, since the magnitude of exothermicity in the fizz zone would increase sharply with increased oxygen in this zone. Further evidence for this mechanism was found in observing the character of the propellant following ignition failure at $p_1$ values below $p_1°$; partial burning was observed to have occurred for the oxygen-deficient igniter systems but never for the oxygen-rich ones, where the propellant was either completely burned or showed no evidence of reaction.

TABLE 3.—DATA ON $\tau_p$, THE IGNITION TIME LAG AS BASED ON A STABLE FLAME OF PROPELLANT *C*, SHOT TUBE I USED WITH THE DETONATION WAVE INTERRUPTED AND SHOT TUBE II USED WITH THE PROPELLANT NONINTERRUPTING

| Shot Tube I, $2H_2$–$O_2$ Igniter | | Shot Tube II, $H_2$–$O_2$ Igniter at $p_1 = 300$ | |
|---|---|---|---|
| $p_1$, lb./sq. in. abs. | $\tau_p$, msec. | Igniter $H_2$–$O_2$, parts by vol. | $\tau_p$, msec. |
| 90 | 170 | 1–1 | 140 |
| 150 | 100 | 3–2 | 200 |
| 150 | 84 | 7–4 | 225 |
| 150 | 66 | 7–4 | 230 |
| 300 | 15 | | |
| 450 | 12* | | |
| 600 | 8* | | |

*Possibly less than given owing to masking of propellant ignition by the detonation shock waves.


## ACKNOWLEDGMENT

Appreciation is expressed to A. S. Filler and W. N. Bryan for assistance in the calculations and some of the experimental work in this paper.


## NOTATION

$p_1$ = initial pressure of the detonating gas igniter
$T_1$ = initial (ambient) temperature of the ignition system
$p_2$ = detonation pressure (hydrodynamic theory)
$T_2$ = detonation temperature
$D$ = detonation velocity
$Q_2$ = heat of explosion
$n$ = number of moles per kilogram of the products of detonation
$p$ = peak pressure measured at the end of the shot tube (approximately twice $p_2$)
$L$ = length
$M$ = momentum or end impulse
$L_m$ = length of propagation of detonation necessary to establish a staeady state detonation
$L'$ = length of propagation from the point of initiation to the point of formation of detonation
$p_1°$ = minimum or threshold (initial) pressure for ignition of the propellant
$\tau_i$ = time lag of initial propellant decomposition
$\tau_p$ = time lag of stable propellant ignition
$d$ = thickness of propellant between pellet ionization pin and surface of propellant pellet
$k$ = burning rate of propellant
$\psi_i°$ = ignition threshold value of the variable $\psi_i$ where $\psi_i$ may be $(O_2)$, $D_2$, $Q_2$, $T_2$, and other detonation functions
( ) indicates that the chemical species enclosed in the brackets was a product of detonation for conditions in the wave front computed thermohydrodynamically.

## LITERATURE CITED


1. Avery, W. H., *J. Phys. & Coll. Chem.*, 54, 917 (1950).
2. Berthelot, D., and H. Gaudechon, *Compt. rend.*, 153, 1220 (1911).
3. Bone, W. A., and D. T. A. Townend, "Flames and Combustion in Gases," p. 163, Longmans, Greene and Co., London and New York (1927).
4. Brian, R. C., and C. A. McDowell, *Trans, Faraday Soc.*, 197, 212 (1949).
5. Chase, C. T., W. H. Smith, Rept. F 2338, Contract DA-36-034-ORD-1105 RD, Franklin Institute, Philadelphia (Oct. 31, 1953).
6. Cook, M. A., *J. Chem. Phys.*, 16, 1081 (1948).

7. Cook, M. A., and F. A. Olson, Tech. Rept. IV, Contract N-123S-80062, Task Order I, Explosives Research Group, Utah University, Salt Lake City (Sept. 15, 1954).
8. Cook, M. A., G. S. Horsley, W. S. Partridge, and W. O. Ursenbach, *J. Chem. Phys.* (to be published).
9. Cook, M. A., and R. T. Keyes, *J. Chem. Phys.* (to be published).
10. Cook, M. A., E. B. Mayfield, and W. S. Partridge, *J. Phys. Chem.* (in press).
11. Cook, M. A., *J. Phys. Chem.* (in press).
12. Crawford, B. L., C. Huggett, and J. J. McBrady, *J. Phys. & Coll. Chem.*, **54**, 854 (1950).
13. Crawford, B. L., and R. G. Parr, *Univ. Minnesota Inst. Technol., Rept.*, **20** (Oct. 10, 1944).
14. Dixon, H. B., *J. Chem. Soc.*, **97**, 662 (1910).
15. Eyring, H., R. E. Powell, G. H. Duffy, and R. B. Parlin, *Chem. Revs.*, **45**, 69 (1948).
16. Gibson, R. E., *J. Phys. & Coll. Chem.*, **54**, 847 (1950).
17. Gordon, W. E., "Third Symposium on Combustion Flame and Explosion Phenomena," p. 579, Williams and Wilkins Co., Baltimore (1949).
18. Jones, E. *Proc. Roy. Soc. (London)*, A198, 523-39 (1949).
19. Jost, W., and H. O. Croft, "Explosion and Combustion Processes in Gases," Chap. V, McGraw-Hill Book Company, Inc. (New York and London) (1946).
20. Kent, R. H., Aberdeen Proving Ground, BRL No. 9 (May, 1935).
21. Kistiakowsky, G. B., H. T. Knight, and M. E. Malin, *J. Chem. Phys.*, **20**, 884 (1952).
22. ———, and P. H. Kydd, *J. Chem. Phys.*, **23**, 271 (1955).
23. ———, and W. G. Zinan, Second ONR Symposium on Detonation, p. 80, Office of Naval Research, Washington, D. C. (February, 1955).
24. Klein, R., M. Menster, G. von Elbe, and B. Lewis, *J. Phys. & Coll. Chem.*, **54**, 877 (1950).
25. Lewis, B., and J. B. Friauf, *J. Am. Chem. Soc.*, **52**, 3905 (1930).
26. Lewis, B., and G. von Elbe, "Combustion Flames and Explosion of Gases," Chap. XI, Academic Press, Inc., New York (1951).
27. Univ. Michigan, Report No. 1 (1951).
28. Naval Ordnance Laboratory, NOLM 10808, White Oak, Md. (July, 1950).
29. Penner, S. S., *J. App. Phys.*, **19**, 278, 392 and 511 (1948).
30. Rice, O. K., and R. Ginnell, *J. Phys. & Coll. Chem.*, **54**, 885 (1950).
31. Rinehart, J. S., and J. Pearson, "Behavior of Metals Under Impulsive Loads," p. 49, American Society for Metals, Cleveland (1954).
32. Wilfong, R. E., S. S. Penner, and F. Daniels, *J. Phys. & Coll. Chem.*, **54**, 863 (1950).

## APPENDIX

The detonation-head model was proposed initially in 1943 in classified reports by one of the authors to account for the observations pertaining to shaped charges with solid explosives. More recently it has been applied to explain various other observations, important among which are velocity-diameter curves (*8* to *11*). It is entirely phenomenalistic in character and, though lacking a fundamental basis, it has proved highly successful as an empirical model for correlating observations, developing new experimental approaches, and solving problems in the design of devices. An important reason for presenting it here is that in reality it is the only model yet available to handle many of the important problems in the technology of detonating explosives. Moreover experience has shown that it provides an intuitive picture of detonation which may be relied upon in predictions of the influence of various geometrical factors, including conditions required for the development of steady state detonations. Here briefly outlined are some of the experimental observations considered most pertinent to the development of the detonation-head model and its essential features.

The total end effect (i.e., the impulse and kinetic energy generated at the end of the charge) applicable, for example, in the formation of jets from shaped charges is adequately described by the following semi-empirical equations:

$$I = F(L)\frac{\pi}{9}\rho_1 (d')^3 W = F(L)\,\pi\,(d')\,p_2/D \qquad \text{(i)}$$

$$T = F(L)\,\pi\,(d')^3\,p_2/12 \qquad \text{(ii)}$$

$$F(L) = 1 - \left(1 - \frac{L}{3.5\,d'}\right)^3;\ \text{for } L < L_m = 1;\ \text{for } L \geqslant L_m \qquad \text{(iii)}$$

where $I$ is the end impulse or momentum, $T$ the effective kinetic energy, $\rho_1$ the charge density, $d'$ the effective diameter (or $d' = (d - d_e)$ where $d_e$, a constant edge effect shown equal to about 0.6 cm. in most solid explosives, is the actual charge diameter), $W$ is the particle velocity calculated for conditions at the Chapman-Jouguet plane, $p_2$ is the "detonation" pressure, and $L$ is the charge length.

Equation (i) to (iii) express the following facts:

1. End effect as measured, for example, by the total hole volume and/or depth of penetration in a homogeneous target of the jet from a shaped charge liner of total mass approximately $M$ increases with charge length, as shown by Equation (ii). That is, end effect increases in proportion to the height of hypothetical truncated cones of constant base diameter $d$ and a height proportional to $L/3.5\ d'$ reaching a maximum (corresponding to a fully developed detonation-head cone) at about 3.5 charge diameters. For $L$ greater than 3.5 $d$ the penetration is independent of $L$.

2. The end impulse varies as the product $\rho_1\ W$ of the explosive, other factors being constant.

3. The total end effect varies as the cube of the effective diameter with other factors constant.

4. Finally, the optimum liner mass for a liner of any angle, shape, and composition is that given approximately by the equation

$$M = F(L)\frac{\pi}{9}\rho_1 (d')^3 \qquad \text{(iv)}$$

That is, the liner should have the same mass as the detonation head.

Equations (i) to (iv) suggest that there exists behind the wave front a detonation head which when fully developed has a mass given approximately by Equation (iv) and a shape resembling approximately a cone of miximum height $d'$. Before it is completely developed, the detonation head appears to resemble truncated cones of height $h = d'(L/3.5d')$ and base diameter $d'$. The outline of this cone,

Fig. i. Flash radiograph of unconfined solid explosive charge (square rather than circular in cross section) showing curved front and "triangular region."

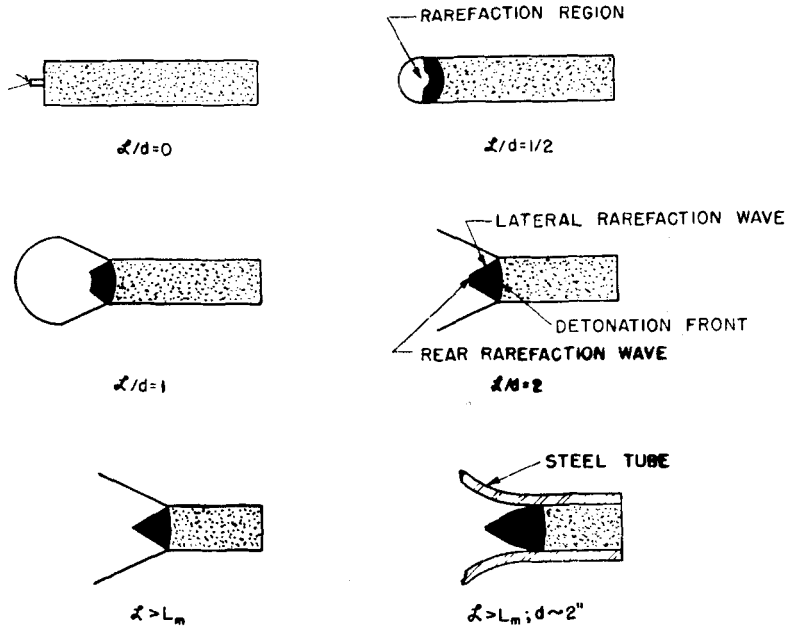


Fig. ii. Development of detonation head and steady state head in unconfined and confined solid explosive charges.

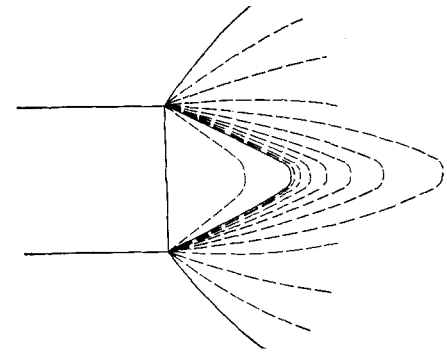

Fig. iii. Schematic representation by constant density contours of pressure gradient in detonation front. (Large distance between contours suggests small gradients, small distance large gradients.)

although not yet completely developed, may be seen vaguely in the flash radiograph of a square cross-sectional charge kindly furnished by Ballistics Research Laboratory, Aberdeen, Maryland, shown in Figure i. A charge of square cross section was used in order to eliminate all variations in X-ray density not associated directly with initial compression as the gases entered the detonation head and with expansion as they left the detonation-head region. This theory is described very briefly, in terms of the essentially equivalent release wave theory of Pugh and associates, by Rinehart and Pearson (*31*).

The detonation-head model proposed to account for these results simply assumes that for many purposes the high-density conical region, sometimes called the "triangular region," in the front of a detonation wave may be regarded as a slug of gas of fairly uniform density and pressure. This region is largely uninfluenced inside its boundaries by rarefactions that move in toward the center from the side of the charge. The fronts of these rarefactions form the boundaries of the detonation head, except for the front boundary, which is the detonation front. According to this model, following initiation of a detonation wave at least the main part of the rarefaction wave moving forward from the rear is assumed to lag somewhat behind and moves at a lower velocity than the wave front. Between the wave front and the front of the main part of the rarefaction region (which is assumed to appear near the stagnation plane, i.e., the region behind the shock front where the particle velocity has finally reached zero), the wave is considered to be approximately a constant density region. For unconfined charges rarefactions moving toward the charge axis from the sides of the charge also are assumed to move forward at speeds lower than the detonation velocity. Figure ii illustrates the apparent development of the head as a function of the charge length, first as a spherical expansion region and later as truncated cones (the base and top being spherical) when the rarefactions start in from the sides; finally, after $L$ becomes equal to or greater than 3.5 $d$, the head is completely formed as a conical region. In order to account for the apparent shape of the detonation head in condensed explosives, one would assign a velocity of about 0.6 $D$ for the front of the main portion of the rarefaction waves from the rear and sides.

One may take into account the hydrodynamic arguments that rarefactions should extend right up to the wave front and still retain the essential features of the detonation-head model by assuming, in accord with conventional hydrodynamics, density gradients (represented in Figure iii by a series of constant density contours equally spaced in density space), small in the region of the detonation head and becoming large only at the boundaries of the detonation head. It is important to realize that experimental evidence argues strongly against very large density gradients in the region designated as the detonation head. Likewise the gradient must be very steep at the boundary of the head (heavy solid line of Figure iii in order to produce the radiographic image. Inside these characteristic boundaries (the lateral rarefaction front or release wave front) rarefactions are thus considered relatively unimportant, but outside they are sufficiently important that momentum and energy cannot be contributed in the direction of propagation by material outside this detonation head. This model should not therefore be regarded as inconsistent with the hydrodynamic concepts that an isentropically spreading rarefaction wave should not have a discontinuous front and that limited rarefactions should extend right up to the wave front; but it merely emphasizes the relative unimportance of these effects within the conical region corresponding to the detonation head determined primarily by the release waves.

This concept has been applied only to a limited extent to gaseous detonations, and experimental evidence showing that it may be applicable to gases confined in heavy walled tubes is limited to the following two observations.

1. After detonation propagates a certain critical distance $L_m$, a steady state momentum is attained in gases just as with solids, except that in solids $L_m$ is only about 3.5$d$, whereas in gases $L_m$ is considerably larger.

2. Direct measurements of the density contours (*22*) of the detonation front in gases appear to show that the density is relatively constant for a distance of about one diameter after the wave has propagated about seven charge diameters from the point of creation of the detonation wave. Facts 1 and 2 are found consistent when one realizes that, owing to a much higher compression ratio, $\rho_2/\rho_1$, in gaseous than in condensed explosives, the stagnation plane should have a velocity in the neighborhood of 0.8$D$ compartd with 0.6$D$ in solids. The reason that the maximum effective length $L_m$ is not infinite or not even excessively large in gaseous detonations in heavy walled tubing is simply that lateral rarefactions or lateral release waves still exist in such gaseous detonations. Instead of being associated with free expansion as in condensed explosives, these lateral release waves result from rapid quenching at the walls of the tube. The important fact shown in this article is that steady state heads are established in gases as well as in condensed explosives.

*Presented at A.I.Ch.E. Louisville meeting*